

Photoacoustic Study of CdS Semiconductor Nanoparticles for Solar Cells Applications

S. Abdallah*, N. Al-Hosiny** and A. Badawi***

*Department of Physics, Taif University, Taif, KSA, and Department of Mathematical and Physical Engineering, Benha University, Cairo, Egypt, dr.saiedabdallah@yahoo.com

**Department of Physics, Taif University, Taif, KSA, nalhosiny@yahoo.co.uk

***Department of Physics, Taif University, Taif, KSA and Physics Department, Ain Shams University, Cairo, Egypt, adaraghmeh@yahoo.com

ABSTRACT

The optical properties and photovoltaic characterization of CdS quantum dots sensitized solar cells (QDSSCs) were studied. CdS QDs were prepared by the chemical solution deposition (CD) technique. Photoacoustic spectroscopy (PA) was employed to study the optical properties of the prepared samples. The sizes of the CdS QDs were calculated using the effective mass approximation (EMA) model gives radii ranged from 1.57 to 1.92 nm, these values are comparable to those obtained by transmission electron microscope (TEM). The current density- voltage (J-V) characteristic curves of the assembled QDSSCs were measured. Fluorine doped Tin Oxide (FTO) substrates were coated with 20 nm-diameter TiO₂ nanoparticles (NPs). Presynthesized colloidal CdS quantum dots of different particles size were deposited on the TiO₂-coated substrates using direct adsorption (DA) method. The FTO counter electrodes were coated with platinum, while the electrolyte containing I⁻/I₃⁻ redox species was sandwiched between the two electrodes. The short current density (J_{sc}) and efficiency (η) increases as the particle size increases. The values of J_{sc} increases linearly with increasing the intensities of the sun light which indicates the greater sensitivity of the assembled cells.

Keywords: CdS quantum dots, photovoltaic, tuning band gap, solar cell.

1 INTRODUCTION

During the last two decades, there has been a great interest in materials science for studying semiconducting quantum dots, since many of their physicochemical properties are substantially different from analogous properties of macroscopic solids [1]. Due to quantum confinement effect, they show size dependent optical, thermal, electrical and photoluminescence properties. Particularly, II-VI semiconductor nanoparticles are currently of great interests for their practical applications in a variety of optoelectronic devices such as, high efficiency thin film transistors, light-emitting diodes [2], electron-beam pumped lasers, electroluminescent devices [3, 4] and

others. CdS quantum dots (QDs) have become a very attractive promising material for many specific applications in solar energy conversion. Special attention has been devoted to investigate the optical and thermal properties to enhance the performance of solar cell devices. Generally, the absorption spectra can be measured by the conventional transmitted intensity method however; samples should be sufficiently thin and have good quality surfaces by pretreatments. This requires samples to be placed in a matrix of transparent material which on the other hand would interfere with the measurements of thermal properties [4]. Photoacoustic (PA) technique is proved to be useful for investigating the optical absorption of opaque samples as well as thermal properties of various materials by measuring the nonradioactive de-excitation processes [5, 6]. There are many methods used to anchor QDs onto the large band gap metal oxides [7-10]. One of these methods is direct adsorption (DA) technique [11].

In this work we utilize PA spectroscopy to investigate the optical properties of CdS QDs to investigate the size quantum confinement effect on the electronic states. CdS QDs were synthesized by chemical deposition (CD) technique. The particles sizes were then estimated using the effective mass approximation (EMA) model, and compared to that measured by transmission electron microscope (TEM). Furthermore, the presynthesized CdS QDs were adsorbed onto TiO₂ NPs by DA technique for different dipping times under ambient conditions. The effect of the CdS QDs size on the QDSSCs characteristic parameters (short circuit current density (J_{sc}), open circuit voltage (V_{oc}), fill factor (FF), and efficiency for energy conversion (η)) were studied.

2 EXPERIMENT

2.1 Preparation of CdS Quantum Dots

Spherical CdS colloidal nanocrystals were prepared by chemical deposition method according to a procedure reported elsewhere. In this procedure, hexadecylamine (HAD) was used as a capping agent together with trioctylphosphine oxide (TOPO) and trioctylphosphine (TOP) to obtain size distribution less than 5%. The sulfur

source such as sodium sulfide (Na_2S) and dimethylcadmium were dissolved of trioctylphosphine (TOP) and rapidly injected into a vigorously stirred mixture of trioctylphosphine oxide (TOPO) and hexadecylamine (HDA). Four samples of different sizes were obtained from the same synthesis at four regular time intervals, during growth labelled (a – d).

2.2 Preparation of Solar Cell Electrodes

A colloidal paste of TiO_2 nanoparticles (NPs) was prepared by the method of G. Syrokostas et al. [12]. Three grams of commercial TiO_2 nanopowder (20 nm) (Degussa P-25 Titanium dioxide consists of 80% anatase and 20% rutile) was ground in a porcelain mortar and mixed with a small amount of distilled water (1 ml) containing acetyl acetone (10% v/v) to create the paste. Finally, a few drops of a detergent (Triton X-100) were added to facilitate the spreading of the paste on the substrate, since this substance has the ability to reduce surface tension, resulting in even spreading and reducing the formation of cracks. The TiO_2 paste was deposited on a conducting glass substrate of $\text{SnO}_2\cdot\text{F}$ (FTO) with sheet resistance of $7 \Omega/\text{sq}$ and $>80\%$ transmittance in the visible region, using a simple doctor blade technique. This was followed by annealing at 450°C for 30 min and the final thickness was $8\mu\text{m}$ after the solvent evaporation. Then the TiO_2 films were dipped into a colloidal solutions of presynthesized CdS QDs, for different dipping times (1, 3, 6, 24, 50 hours) to form five working electrodes. The counter electrodes were prepared by coating another FTO substrate sheet of resistance of $7 \Omega/\text{sq}$ with Pt.

2.3 Assembly of QDSSC

Both of the working and counter electrodes were assembled as a sandwich type cell using clamps. Then they were sealed by using a hot-melt polymer sheet (solaronix, SX1170-25PF) of $25 \mu\text{m}$ thickness in order to avoid evaporation of electrolyte. Finally, Iodide electrolyte was inserted in the cell with a syringe, filling the space between the two electrodes.

2.4 Measurements

The absorption spectra of CdS QDs were recorded by PA technique. The light beam from xenon lamp was focused into the entrance slit of a monochromator. The output beam of the exit slit was mechanically modulated by an optical chopper, and focused onto the sample which was mounted inside a PA cell (MTEC Model 300). The sound wave generated from the sample can be subsequently detected as an acoustic signal by a highly sensitive electrical microphone fixed in the PA cell. The PA signal was then amplified using a lock-in amplifier. A personal computer was interfaced to the system for automatic data acquisition and analysis. The PA spectra were compared to those obtained by a regular UV-Vis absorption (JASCO V-

670). The particle sizes were estimated directly using TEM and confirmed by PA spectra. The CdS QDSSCs were subjected to the illumination of a solar simulator (ABET technologies, Sun 2000 Solar Simulators, USA) operating at $100 \text{ mW}/\text{cm}^2$ (AM 1.5). The current density–voltage (J–V) characteristics for CdS QDSSCs of different dipping time were recorded with a Keithley 2400 voltage source/ammeter. The intensity of the incident solar illumination was adjusted to 1 sun condition using a Leybold certified silicon reference solar cell (Model: [57863]). A J-V characteristic curves of QDSSC were recorded at various illumination intensities using attenuators and calibrated by the previous Si reference solar cell. All experiments were carried out under ambient conditions.

3 RESULTS AND DISCUSSION

3.1 Optical Absorption Measurements

The average particle radii of the synthesized CdS QDs were estimated using transmission electron microscope (TEM), which approximately ranged from 1.5 nm for sample a to 2.0 nm for sample d. The TEM images of sample a and d are shown in Fig.1 (a and b) respectively.

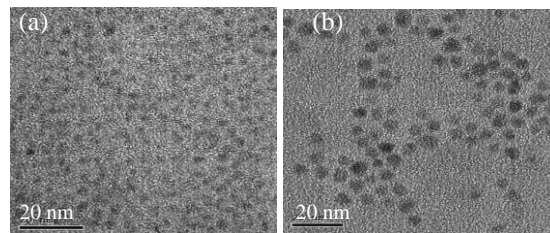


Fig. 1:(a) TEM micrograph for sample a, and (b) TEM micrograph for sample d.

The PA spectra for the four samples of CdS QDs (a–d) as a function of the wavelength of the incident beam at a constant modulation frequency of 15 Hz are shown in Fig. 2(a). The PA spectra for all samples are normalized using the PA spectrum obtained for carbon black in the allowed region of the used xenon lamp. The absorption edges varies between 394 nm for sample a to 432 nm for sample d. It is easily observed that there is a red shift towards lower energy region with increasing the size. This behavior is attributed to the quantum confinement effect. The calculated energy band gap ($E_g = hc / \lambda$) for the same samples varies between 3.15 eV for sample a to 2.88 eV for sample d. The optical absorption spectra of the same samples in colloidal solution were also obtained by regular UV-Vis absorption and given in Fig. 2 (b). Although, the UV-Vis. spectra are for samples in colloidal form, and the PA spectra are for powder form, the two spectra gave peaks that are very close. The slight difference in the absorption edges positions of CdS QDs between PA and UV-Vis. spectra may be due to the character of the acoustic wave in PA and the photonic character of the UV-Vis.

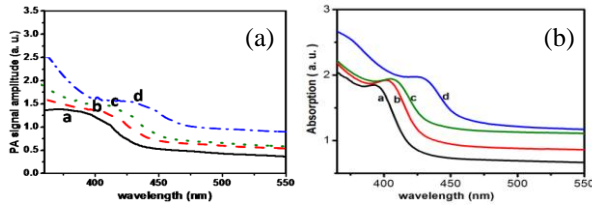


Fig. 2: (a) Normalized PA spectra for the four CdS QDs samples, (b) UV-Vis. Absorption spectra for CdS QDs samples.

Furthermore, the sizes of the synthesized CdS QDs were also estimated using EMA model which is given as[13, 14]:

$$E_{g(nano)} = E_{g(bulk)} + \frac{\hbar^2}{8R^2} \left(\frac{1}{m_e} + \frac{1}{m_h} \right) - \frac{1.8e^2}{4\pi\epsilon\epsilon_0 R} - \text{small terms} \quad (1)$$

Where $E_{g(bulk)} (=2.482 \text{ eV})$ [15] is the bulk CdS crystal band gap value, $E_{g(nano)}$ is the nano crystal band gap value, R is the radius of CdS QDs, m_0 is mass of electron, $m_e (=0.2 m_0)$ [15] and $m_h (=0.7m_0)$ [15] are the electron and hole effective masses respectively, ϵ_0 the permittivity of vacuum and $\epsilon (=5.29)$ [15] is the relative dielectric constant for CdS. The values of $E_{g(nano)}$ that obtained from PA spectra together with equation 1 are used to calculate the average radii of CdS QDs. The values of radii are ranging from 1.57 nm for sample a to 1.92 nm for sample d, which are comparable to those obtained by TEM images.

3.2 Characterization of CdS QDs Sensitized TiO₂ Electrodes

The UV-Vis. absorption spectra of the working electrodes for all CdS QDs sizes were recorded for different dipping times (1, 3, 6, 24, and 50 hour). As an example, figure 3 shows the absorption spectra of CdS QDs (sample d) sensitized TiO₂ electrodes. It is clearly seen that as the dipping time increases the absorption increases indicating an increased adsorption amount of CdS QDs. Furthermore, a significant shift toward the visible spectra region is also observed.

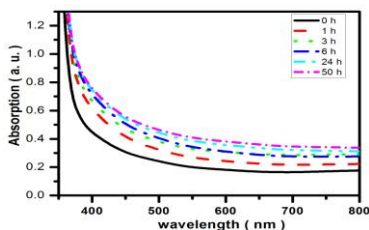


Fig. 3: UV-Vis. Absorption spectra of CdS QDs (sample d) / TiO₂ electrode at different dipping times.

3.3 Characterization of CdS QDSSC

The J-V characteristics curves of the assembled CdS (sample d) QDSSCs for the five dipped times (1 h, 3 h, 6 h,

24 h, and 50 h) are shown in Fig. 4 using TiO₂ photoelectrodes and 100 mW/cm² from a solar simulator.

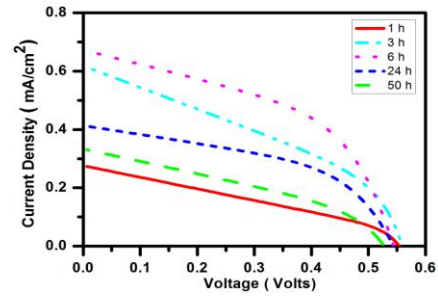


Fig. 4: J-V Characteristics curves of CdS (sample d) QDSSCs for: (a) 1 h, (b) 3 h, (c) 6 h, 24h, and (d) 50 h dipping time.

The values of V_{oc} , J_{sc} , FF, and η of the assembled QDSSCs at different dipping time are given in table 1. It is observed that both J_{sc} and η increase as the dipping time increases up to 6 hours, peaking at 0.67mA/cm² and 0.18% respectively. These values lowered down again to 0.41 to mA/cm² and 0.11 % for 24 h and 0.33mA/cm² and 0.06% for 50 hours dipping time. All other CdS QDs sizes showed the same behavior. These results could be explained in term of; as the dipping time increases more than 6 hours, an additional amount of CdS QDs is loaded, leading to block the nanopores of TiO₂ layer, causing the reduction of both J_{sc} and η .

Dipping time (h)	V_{oc} (Volt)	J_{sc} (mA/cm ²)	FF	(%)
1	0.56	0.27	0.32	0.05
3	0.56	0.62	0.37	0.13
6	0.54	0.67	0.50	0.18
24	0.54	0.41	0.49	0.11
50	0.53	0.33	0.34	0.06

Table 1: J-V Characteristics parameters of CdS (sample d) QDSSCs for different dipping times.

Fig. 5 shows the J-V characteristics of the assembled CdS QDSSCs constructed from different sizes of CdS QDs (with radii 1.57, 1.64, 1.69, and 1.92 nm) at 6 hours dipping time under 1.5 AM illumination from ABET solar simulator. The extracted characteristics parameters are given in table 2.

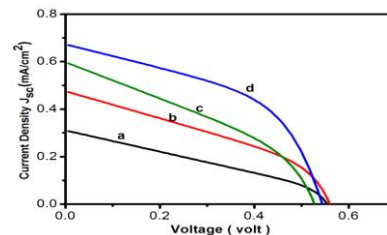


Fig. 5: J-V Characteristic curve of QDSSCs of CdS QDs radii : (a) 1.57, (b) 1.64, (c) 1.69, and (d) 1.92nm.

QDs Size (nm)	QD Band Gap (eV)	V _{oc} (Volt)	J _{sc} (mA/cm ²)	FF	(%)
1.57	3.15	0.55	0.31	0.31	0.05
1.64	3.09	0.56	0.47	0.37	0.09
1.69	3.04	0.53	0.60	0.36	0.11
1.92	2.89	0.54	0.67	0.50	0.18

Table 2: J-V Characteristics parameters of CdS QDSSCs for different QDs sizes, at 6 hr dipping time and 1 sun.

It is clearly seen that as CdS QDs size increases, the values of J_{sc} and η increase. The maximum values of J_{sc} and η are 0.67 mA/cm² and 0.18% respectively for the biggest CdS QDs size (sample d). This result could be explained as follows: Increasing the particle size results in a red shift and thus causes relatively high absorption of the incident photon from solar spectrum. Therefore, CdS QDs of radius 1.92 nm (correspond to 432 nm) harvest more visible photon than the other particle sizes. Furthermore, It is seen that V_{oc} is independent on CdS QDs size, since the electrons injected quickly from the CBM of CdS QDs to the lowest CB energy of TiO₂ NPs, indicating that the CB level of TiO₂ NPs and the VB of the electrolyte dictate Voc of the assembled QDSSCs. Additionally, DA technique which we used to deposit CdS QDs onto TiO₂ NPs lead to pin directly the CdS QDs bands to that of TiO₂ NPs without any barriers, which causes a direct electronic interaction between the two semiconductor materials (CdS QDs and TiO₂ NPs). So, DA technique minimizes the electrons' injection time from CBM of CdS QDs to that of TiO₂ NPs.

The performance of the assembled CdS (sample d) QDSSCs with various intensities of solar illumination (from 0 - 100% sun) are given in fig.6. It is seen that as the intensity of the incident light increases, the measured J_{sc} increases linearly due to increased injected electrons. The approximately constant value of Voc indicate the relative sensitivity of CdS QDSSCs that is prepared by DA method.

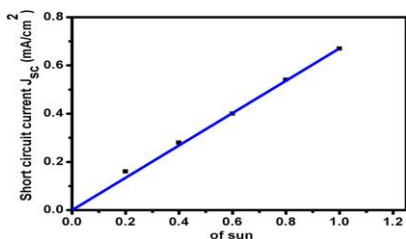


Fig.6: Short circuit current density (J_{sc}) vs. percentage of sun.

4 CONCLUSIONS

The nondestructive PA technique has been used to study the optical absorption spectra of CdS QDs of different sizes. The spectra shifted to lower energy region with

increasing the particle size. The PA spectra were compared with regular UV-Vis absorption which gives comparable results. These CdS QDs of different sizes were deposited onto TiO₂ NPs using DA technique by varying dipping time (0 to 50 hours) to serve as a sensitizer for photovoltaic cell. Our results show that DA technique is a suitable method to adsorb CdS QDs onto TiO₂ nanoparticles up to 50 hours without use of linkers. The values of J_{sc} and η increase as the QDs size increases. Such an increase is mostly attributed to the consistence with the incident solar intensity spectrum. Furthermore, as the intensity of the incident solar light increases, J_{sc} increases linearly, indicating greater sensitivity of CdS QDSSCs.

5 ACKNOWLEDGMENTS

The authors wish to thank Taif University for the grant research No. (1/432/1110). The Quantum Optics Research Group (QORG) at Taif University is also thanked for their assistance during this work.

REFERENCES

- [1] B. Pejova, A. Tanuševski and I. Grozdanov, Journal of Solid State Chemistry, 177, 4785-4799, 2004.
- [2] P.K. Khanna and N. Singh, Journal of Luminescence 127, 474-482, 2007.
- [3] P. Guyot-Sionnest, C. R. Physique, 9, 777-787, 2008.
- [4] T.A. El-Brolossy, et al., Eur. Phys. J. Special Topics, 153, 365-368, 2008.
- [5] S.D. George, et al., phys. stat. sol. (A), 196, 384-389, 2003.
- [6] M.A. Gonzalez-T, A. Cruz-Orea and M.d.L.A.-A.F.d.L. Castillo-A, Thin Solid Films, 480-481, 358-361, 2005.
- [7] A. Tubtintae, et al., Electrochemistry Communications, 12, 1158-1160, 2010.
- [8] I.a. Mora-Seró, et al., Nanotechnology, 19, 424007, 2008.
- [9] A. Salant, et al., ACS NANO, 4, 5962-5968, 2010.
- [10] P.V. Kamat, J. Phys. Chem. C, 112, 18737-18753, 2008.
- [11] S. Giménez, et al., Nanotechnology, 20, 295204, 2009.
- [12] G. Syrokostas, M. Giannouli and P. Yianoulis, Renewable Energy, 34, 1759-1764, 2009.
- [13] B. Pejova and I. Grozdanov, Materials Chemistry and Physics, 90, 35-46, 2005.
- [14] M. Thambidurai, et al., Chalcogenide Letters, 6, 171 - 179, 2009.
- [15] O. Madelung, Semiconductors : Data Handbook, 3rd ed., Springer-Verlag, Berlin, 2004.